Geomechanics and Engineering, *Vol. 42, No. 5 (2025) 397-407*
https://doi.org/10.12989/gae.2025.42.5.397

Experimental and computational mathematics for vibration in concrete beams containing nanoparticles based mathematical modelling

Hongying Si*[1], M. Alizadeh[2] and T. Marmy[3]

[1]*School of Mathematics and Statistics, Shangqiu Normal University, Shangqiu, Henan, China, 476000*
[2]*Department of Civil Engineering, Khor.C., Islamic Azad University, Khorramabad, Iran*
[3]*Department of Mechanical Engineering, University of Zabol, Zabol, Iran*

(*Received February 12, 2024, Revised August 26, 2025, Accepted September 1, 2025*)

Abstract. In this work, computational mathematics framework demonstrates the analysis of vibration in nanoparticle-reinforced concrete beams via superior mathematical modeling. It derives a sinusoidal shear deformation beam theory (SSDBT) continuum mechanics model that is higher-order model with exact or true geometrical nonlinearity. A stochastic homogenization problem that models probabilistic agglomeration of the nanocomposite is used to derive its effective properties based on Mori-Tanaka micromechanics. The equations that govern this situation, as a partial differential equation, are obtained as a result of the variational calculus (also known as Hamilton principle) and expressed as an eigenvalue problem by means of the precise analytic techniques. To validate the accuracy of the proposed model, experimental studies are conducted to compare compressive strength. Since GO nanoparticles typically do not readily disperse in water, a thorough dispersion process is employed prior to concrete sample production. This involves utilizing a combination of mechanical shaking, magnetic stirring, ultrasonic treatment, and mechanical mixing. Computational mathematic algorithm is used to ensure the resulting transcendental frequency equation is sufficiently solved. In order to validate its model, the model is compared with the results obtained in the experiment as a benchmark case of the numerical solutions. The mathematical model is impressive in its predictive accuracy because the measured experimental data on compressive strength. The compressive strength exhibit a close alignment with the mathematical model and existing literature, with a maximum difference of 1.25%. The use of mathematical modeling, which forms the core of this study, has established a formal analytical mechanism to determine the vibrational characteristics and reduces the need for costly experimental trials in designing high-performance nanocomposite structures.

Keywords: analytical method; concrete beam; experimental; GO nanoparticles; vibration

1. Introduction

Nanotechnology has resulted in the creation of nano-engineered composite materials that possess increased mechanical properties, which made the relevance of nano-engineered materials even greater in structural applications. The modelling can be divided into two categories of atomic modeling and continuum mechanics (Chen *et al.* 2025, Cui *et al.* 2024, Deng *et al.* 2022, 2024, Gong and Li 2024). More interesting developments that have made concrete notable advances in the improvement of its mechanical properties including sole enhancement of stiffness and strength directly impacting the dynamic response of concrete elements includes the addition of nanoparticles to the cementitious matrices (Tang *et al.* 2025, Yao *et al.* 2023, 2025, Zhang *et al.* 2023a, b). An example of such nanoparticles is the nanoparticle graphene oxide (GO) (Chen *et al.* 2020, Hong *et al.* 2020, Wu *et al.* 2020, Zhang *et al.* 2025).

New developments over nanomaterials have exhibited drastic impact on the mechanical ability and capacities of composite structures and concrete materials (He *et al.* 2024, Huang *et al.* 2022, Liu *et al.* 2024, Niu *et al.* 2024, Prakash *et al.* 2025). A number of works have been devoted to the reinvention of the composite materials of nanoscale reinforcements, e.g., carbon nanotubes (CNTs), graphene, and nano-SiO_2 synthesized and incorporated into the traditional materials to enhance strength, durability, and multi-functionality (Sun *et al.* 2017, Tang *et al.* 2025, Wang *et al.* 2023, 2025, Yang *et al.* 2024). A multiscale analysis was made on the deflection and stress distribution of nanocomposite reinforced beams (Wuite and Adali 2005) which showed the positive impact of nano-reinforcements. Their publication formed a basis of knowledge in structural usage of nanocomposites. Rafiee *et al.* (2009) investigated the strengths of the graphene-reinforced nanocomposites when it comes to fracture and fatigue resistances. The outstanding mechanical property of graphene was also a significant contributor to augmented durability implying that graphene could be used in the manufacture of high-performance materials. Liew *et al.* (2014) have studied the stability and the postbuckling of carbon nanotube reinforced functionally graded cylindrical panel under the compression load in the axis of the panel by adopting a meshless computational method. Their study established a better loading ability and increase stability of the nanocomposite panels because of the graded distribution of the CNTs. Azandariani *et al.* (2022) presented a spectral element

*Corresponding author, Ph.D.
E-mail: sihongying@sqnu.edu.cn

ISSN: 2005-307X (Print), 2092-6219 (Online)

procedure to discuss the axially-loaded functionally graded beams based on the first-order shear deformation theory, which provides effective and precise vibration solution of complex grading patterns. The vibration characteristics of nano-reinforced structures have attracted quite some level of interest in recent years, with a number of theoretical and methodological modeling options being put forward. To give an example, Gholami *et al.* (2023) have developed a dynamic stiffness approach to analyze the free vibration of bi-directional functionally graded (BFG) Timoshenko nanobeams and therefore this tool can be used as a highly accurate method of study in the nano-level dynamic field of study. This was taken further by Zare *et al.* (2024) to nonlocal, nonlinear free vibration analysis of BFG Timoshenko nanobeams that demonstrated the significance of scale-dependent behavior when studying nanostructures. Setayesh *et al.* (2024) examined the response of forced vibration of relatively-thick carbon nanotube (CNT)-reinforced composite plates in the larger context of forced vibration of nanocomposite structures, where it was shown that when the reinforcement is at nanoscale, the dynamic stiffness and damping properties change significantly. Next, Hamzehkhani *et al.* (2024) focused on the bending vibrations of pre-twisted sandwich beams by precisely formulating a dynamic stiffness matrix representation, and the effect of layered systems is evident in such vibrations. Labaran *et al.* (2024) performed an experiment, researching how the concrete strength, durability, and cost-efficiency are changed by the addition of nano-silica, finding that the performance indicators were improved dramatically. Cheng *et al.* (2025) used the numerical model of AI-integrated to calculate the nonlinear post-buckling of the Mindlin composite plate reinforced with the functionally graded carbon nanotube, and suggested the sophisticated skills of simulations of the complicated behavior of nanocomposites. New studies on the stability of sustainable infrastructure have emerged by looking at concrete that has been nano-engineered. Multifunctional construction materials Song *et al.* (2025) used experimental and numerical modeling to enable optimal energy extraction using smart nano-engineered concrete. Hailin Jia *et al.* (2025) modeled and tested the idea of thermal insulation model of nano-SiO2 foam concrete and vacuum insulation panel sandwich on building exterior surfaces that showed higher benefits of thermal performance. A study by Su *et al.* (2025) examined how nano-SiO2 and nano-CaCO3 can be incorporated into concrete in combination, saying the result was better abrasion resistance and a finer microstructure. Verma *et al.* (2025) have evaluated different methods of dispersion of nano-SiO2 in concrete matrices, at the same time mentioning that the successful dispersion of the nano-particles in uniform distribution of nano-particles is assumed to lead to best outcomes. A thorough review of nano-engineering progress in cement and concrete was presented by Barbhuiya *et al.* (2025), summarizing a state of the art research on progress and future directions.

Latest development in the field of structural and material engineering has resulted in a dotted research to enhance the mechanical and dynamic behavior of concrete-based and composite structures through emerging techniques on reinforcement, modeling and addition of advanced materials like nanomaterials, and fibers. The study conducted by Zhai *et al.* (2025), the vibration response of a composite, doubly-curved, shell with damping layers with a view to structural damping was able to attain a better dynamic behavior. Yang *et al.* (2025a,b) comprehensively studied how to predict the restrained stress in ultra-high-performance concrete (UHPC) by correlating long- and in-situ creep behaviors, and provided a proper long-term and in-situ stress prediction model with increased accuracy of long-span and prestressed buildings. The paper by Sun *et al.* (2017) evaluated the vibration velocity of the X-section cast in place concrete (XCC) pile-raft foundations of ballastless tracks and offered the knowledge about the foundation dynamics based on railway loading. As it can be seen in Niu *et al.* (2024), neural network methods were used to model damage of concrete cement under compression; the accuracy was found to be high, and the methods used have continued to present robust potential in the use of smart structural health monitoring. The effects of fiber complexity specifically were the prospective results provided by Gao *et al.* (2025) that considered uniaxial tensile stress-strain characteristics in regard to 3D/4D/5D fibers reinforced by steel to produce an enhanced mechanical behavior. Zhang *et al.* (2025) provide a comprehensive perspective on the cohesive zone modeling of the interface bond phenomenon wherein the effect of fiber-reinforced polymer (FRP) and concrete was established. A practical use of the findings has been given by Huang *et al.* (2022) as they explored seismic behavior of reinforced concrete columns that have been augmented under combined lateral and axial load. This literature provided an in-depth overview of nanomaterial-modified alkali-activated composites written by Zhang *et al.* (2023) with a focus on their fresh, mechanical, and microstructural properties. In reference to this, Yao *et al.* (2023) tested the cyclic behavior of new beam-to-column connections with small buttress sections of fuse elements instead of the beam sections proposed to provide greater levels of energy dissipation and structural resilience during seismic action.

In spite of all this, study of the vibrational performance of GO-reinforced concrete beams has not been studied fully and more specifically, the dispersive quality and agglomeration effects are not considered in the study directly. This is because the model or theory presented in the current paper endeavors to fill this gap by modeling the vibration properties of GO nanoparticle-reinforced concrete beams using the SSDBT and the Mori Tanaka model homogenization method. The compressive strength data is used to validate the model and the influence of GO content, agglomeration, boundary condition, temperature, moisture, and geometric parameters occurring on natural frequency are studied.

2. Mathematical modeling

Fig. 1 presents a concreting the reinforcement of graphene oxide nanoparticle inserted into the conventional cementitious substance posing an implementation of the

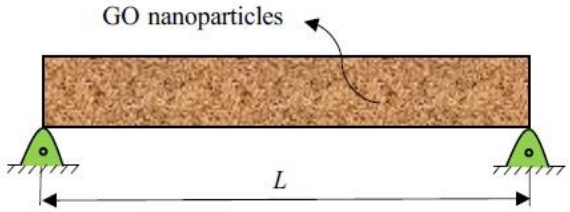

Fig. 1 Schematic of a concrete beam reinforced with GO nanoparticles

nano substances in the standard cementitious concrete. The diagram provides accentuation of the even distribution of GO nanoparticles in an actual concrete which is essential to improve the mechanical properties of the beam like stiffness, strength and durability. Inclusion of GO nanoparticles also enhances load-bearing not only but also leads to improved crack resistance and damping behavior under dynamic loading. This figure gives a visual description of nanotechnology and how it may be utilized in an effective manner to create high-performance structural components in the field of high end civil engineering.

Based on SSDT, the displacement field is (Thai and Vo 2012)

$$u_1(x,z,t) = u(x,t) - z\frac{\partial w(x,t)}{\partial x} + f\psi(x,t) \tag{1}$$

$$u_2(x,z,t) = 0 \tag{2}$$

$$u_3(x,z,t) = w(x,t) \tag{3}$$

where u_1, u_2 and u_3 are the mid-plane deflections in the axial, transverse and thickness directions, respectively; ψ represents the rotation of cross section about y axis; $f = \frac{h}{\pi}\sin\left(\frac{\pi z}{h}\right)$. Using Eqs. (1) to (3), the nonlinear strain-displacement relations based on Von -Karman theory are as follows

$$\varepsilon_{xx} = \frac{\partial u}{\partial x} - z\frac{\partial^2 w}{\partial x^2} + f\frac{\partial \psi}{\partial x} \tag{4}$$

$$\varepsilon_{xz} = cos\left(\frac{\pi z}{h}\right)\psi \tag{5}$$

The stress relations for the proposed structure are

$$\sigma_{xx} = Q_{11}(\varepsilon_{xx} - \alpha_{xx}T - \beta_{xx}C) \tag{6}$$

$$\sigma_{xz} = Q_{55}\varepsilon_{xz} \tag{7}$$

where T and C are temperature and moisture changes, respectively; α_{xx} and β_{xx} are thermal and moisture coefficient, respectively.

2.1 Mori-Tanaka model

Here, E and ν are Young's modulus and Poison's ratio of the GO-reinforced concrete beam which are

$$E = \frac{9KG}{3K+G} \tag{8}$$

$$\upsilon = \frac{3K-2G}{6K+2G} \tag{9}$$

where the effective bulk modulus (K) and effective shear modulus (G) may be expressed as

$$K = K_{out}\left[1 + \frac{\xi\left(\frac{K_{in}}{K_{out}} - 1\right)}{1 + \alpha(1-\xi)\left(\frac{K_{in}}{K_{out}} - 1\right)}\right], \tag{10}$$

$$G = G_{out}\left[1 + \frac{\xi\left(\frac{G_{in}}{G_{out}} - 1\right)}{1 + \beta(1-\xi)\left(\frac{G_{in}}{G_{out}} - 1\right)}\right], \tag{11}$$

where

$$G = G_{out}\left[1 + \frac{\xi\left(\frac{G_{in}}{G_{out}} - 1\right)}{1 + \beta(1-\xi)\left(\frac{G_{in}}{G_{out}} - 1\right)}\right], \tag{12}$$

$$K_{out} = K_m + \frac{C_r(\delta_r - 3K_m\chi_r)(1-\zeta)}{3[1-\xi-C_r(1-\zeta)+C_r\chi_r(1-\zeta)]}, \tag{13}$$

$$G_{in} = G_m + \frac{(\eta_r - 3G_m\beta_r)C_r\zeta}{2(\xi - C_r\zeta + C_r\zeta\beta_r)}, \tag{14}$$

$$G_{out} = G_m + \frac{C_r(\eta_r - 3G_m\beta_r)(1-\zeta)}{2[1-\xi-C_r(1-\zeta)+C_r\beta_r(1-\zeta)]}, \tag{15}$$

where two parameters ξ and ζ describe the agglomeration of nanoparticles and C_r is relates to the SiO_2 volume fraction. In addition, $\chi_r, \beta_r, \delta_r, \eta_r$ may be calculated as

$$G_{out} = G_m + \frac{C_r(\eta_r - 3G_m\beta_r)(1-\zeta)}{2[1-\xi-C_r(1-\zeta)+C_r\beta_r(1-\zeta)]}, \tag{16}$$

$$\beta_r = \frac{1}{5}\left\{\begin{array}{l}\frac{4G_m + 2k_r + l_r}{3(k_r + G_m)} + \frac{4G_m}{(p_r + G_m)} \\ + \frac{2\left[G_m(3K_m + G_m) + G_m(3K_m + 7G_m)\right]}{G_m(3K_m + G_m) + m_r(3K_m + 7G_m)}\end{array}\right\}, \tag{17}$$

$$\delta_r = \frac{1}{3}\left[n_r + 2l_r + \frac{(2k_r - l_r)(3K_m + 2G_m - l_r)}{k_r + G_m}\right], \tag{18}$$

$$\eta_r = \frac{1}{5}\left[\begin{array}{l}\frac{2}{3}(n_r - l_r) + \frac{4G_m p_r}{(p_r + G_m)} \\ + \frac{8G_m m_r(3K_m + 4G_m)}{3K_m(m_r + G_m) + G_m(7m_r + G_m)} \\ + \frac{2(k_r - l_r)(2G_m + l_r)}{3(k_r + G_m)}\end{array}\right]. \tag{19}$$

where k_r ، l_r ، n_r ، p_r and m_r are the Hills elastic modulus for the nanoparticles (Mori and Tanaka 1973); K_m and G_m are the bulk and shear moduli of the matrix which can be written as

$$K_m = \frac{E_m}{3(1-2\upsilon_m)} \tag{20}$$

$$G_m = \frac{E_m}{2(1+\upsilon_m)} \tag{21}$$

where $E_m$and υ_m are Young's modulus and the Poisson's rat io of concrete beam, respectively. Furthermore, β, α can be obtained from

$$\alpha = \frac{(1+\upsilon_{out})}{3(1-\upsilon_{out})} \tag{22}$$

$$\beta = \frac{2(4-5\upsilon_{out})}{15(1-\upsilon_{out})} \tag{23}$$

$$\upsilon_{out} = \frac{3K_{out}-2G_{out}}{6K_{out}+2G_{out}} \tag{24}$$

2.2 Governing equations

One of the ways to obtain the governing equations is energy method and the principle of Hamilton. When formulating the governing equations, use of the Hamilton principle was selected on grounds of appropriateness and applicability in complicated composite structures that have coupled fields and use higher-order deformation theory (as is the case in SSDBT, employed in this work). In contrast to other techniques, like Newtonian or Lagrangian mechanics, Hamilton principle can be used in the case when both potential and kinetic energies are considered by allowing both of them to be added together, it has also been useful in the derivation of variational equations of systems with distributed parameters. This application is especially good in nano-reinforced composite cases where nonlinearities, shear deformation and coupling are of importance. Moreover, Hamilton principle has found common application in comparable studies on composite and nanostructures, which provide mathematical continuity and semantic in obtaining partial differential equations of description of dynamic behavior. Potential energy of structure can be written as follows

$$U = \frac{1}{2}\int_V (\sigma_{xx}\varepsilon_{xx} + \sigma_{xz}\varepsilon_{xz})\, dV \tag{25}$$

By replacing Eqs. (4) and (5) into Eq. (25), potential energy is

$$U = \frac{1}{2}\int_V \left(\sigma_{xx}\left(\frac{\partial u}{\partial x} - z\frac{\partial^2 w}{\partial x^2} + f\frac{\partial \psi}{\partial x}\right) + \sigma_{xz}\left(cos\left(\frac{\pi z}{h}\right)\psi\right)\right) dV. \tag{26}$$

The plane forces and moments can be defined as

$$(N, M, P) = \int_A (1, z, f)\sigma_x\, dA \tag{27}$$

$$Q = \int_A cos\left(\frac{\pi z}{h}\right)\sigma_{xz}\, dA \tag{28}$$

Hence, the potential energy is

$$U = \int_x \left(N\frac{\partial u}{\partial x} - M\frac{\partial^2 w}{\partial x^2} + P\frac{\partial \psi}{\partial x} + Q\psi\right) dx \tag{29}$$

The kinetic energy is

$$K = \frac{\rho}{2}\int \left(\dot{u_1}^2 + \dot{u_2}^2 + \dot{u_3}^2\right) dV \tag{30}$$

By replacing Eqs. (1)-(3) into Eq. (30) we have

$$K = \frac{\rho}{2}\int \left(\left(\frac{\partial u}{\partial t} - z\frac{\partial^2 w}{\partial x \partial t} + f(z)\frac{\partial \psi}{\partial t}\right)^2 + \left(\frac{\partial w}{\partial t}\right)^2\right) dV \tag{31}$$

where ρ is the density of the structure. The inertia moment can be defined as

$$\begin{Bmatrix} I_0 \\ I_1 \\ I_2 \\ I_3 \\ I_4 \\ I_5 \end{Bmatrix} = \int \begin{bmatrix} \rho \\ \rho z \\ \rho z^2 \\ \rho f(z) \\ \rho z f(z) \\ \rho f(z)^2 \end{bmatrix} dA \tag{32}$$

Hence, we have

$$K = 0.5\int \left[I_0\left(\left(\frac{\partial u}{\partial t}\right)^2 + \left(\frac{\partial w}{\partial t}\right)^2\right) - 2I_1\left(\frac{\partial u}{\partial t}\frac{\partial^2 w}{\partial x \partial t}\right) + I_2\left(\frac{\partial^2 w}{\partial x \partial t}\right)^2 - 2I_3\left(\frac{\partial u}{\partial t}\frac{\partial \psi}{\partial t}\right) - I_4\left(\frac{\partial^2 w}{\partial x \partial t}\frac{\partial \psi}{\partial t}\right) + I_5\left(\frac{\partial \psi}{\partial t}\right)^2\right] dx \tag{33}$$

Hamilton's principle is stated as

$$\int_0^t (\delta U - \delta K) dt = 0 \tag{34}$$

Hence, the governing equations are

$$\delta u: \frac{\partial N}{\partial x} = I_0\frac{\partial^2 u}{\partial t^2} - I_1\frac{\partial^3 w}{\partial x \partial t^2} - I_3\frac{\partial^2 \psi}{\partial t^2} \tag{35}$$

$$\delta w: \frac{\partial^2 M}{\partial x^2} - \frac{\partial^2 F}{\partial x^2} + \frac{\partial Q}{\partial x} = I_0\frac{\partial^2 w}{\partial t^2} + I_1\frac{\partial^3 u}{\partial x \partial t^2} - I_2\frac{\partial^4 w}{\partial x^2 \partial t^2} + I_4\frac{\partial^3 \psi}{\partial x \partial t^2} \tag{36}$$

$$\delta \psi: Q_x - \frac{\partial F_x}{\partial x} = I_5\frac{\partial^2 \psi}{\partial t^2} - I_3\frac{\partial^2 u}{\partial t^2} + I_4\frac{\partial^3 w}{\partial x \partial t^2} \tag{37}$$

By substituting Eqs. (6) and (7) into (27) and (28), the internal forces and moments are

$$N = hQ_{11}\frac{\partial u}{\partial x} \tag{38}$$

$$M = -Q_{11}I\frac{\partial^2 w}{\partial x^2} + \frac{24Q_{11}I}{\pi^3}\frac{\partial \psi}{\partial x} \tag{39}$$

$$P = -\frac{24Q_{11}I}{\pi^3}\frac{\partial^2 w}{\partial x^2} + \frac{6Q_{11}I}{\pi^2}\frac{\partial \psi}{\partial x} \tag{40}$$

$$Q = \frac{Q_{55}A}{2}\psi \tag{41}$$

where

$$(A, I) = \int_A (1, z^2)dA \tag{42}$$

3. Analytical solution

Being constrained by a simply supported condition, the connecting final three mode shapes of the beam can be mathematically written so that they are sinusoidal functions, in that they are closed-form solutions of the associated governing differential equation of motion in transverse vibrations of a beam under pure simply supported boundary conditions. These mode shapes define the typical shapes of deformation that the beam will take at particular natural frequencies and each mode will be defined at a higher frequency and differ in complexity of the shape. Both Ends of the beams in simply supported beam is free to rotate and does not have the ability of resisting the moments and thus the displacement of the supports is "zero". The modes proceeds; appropriately, and will be the Sine-functions such as fulfill these border conditions, and can be expressed as

$$d = \begin{Bmatrix} u \\ w \\ \psi \end{Bmatrix} = \sum_{m=0}^{\infty} \begin{Bmatrix} A_1 \cos(\frac{m\pi x}{L})e^{i\omega t} \\ A_2 \sin(\frac{m\pi x}{L})e^{i\omega t} \\ A_3 \sin(\frac{m\pi x}{L})e^{i\omega t} \end{Bmatrix}, \tag{43}$$

where ω represents vibration frequency of the beam, m is axial wave numbers. Replacing Eq. (43) into motion equations yields

$$[K][d] + [M][\ddot{d}] = 0 \tag{44}$$

where $[K]$ and $[M]$ are stiffness and mass matrixes, respectively. By using the eigenvalue technique, natural frequency of the structure can be calculated through solving the characteristic equation, which is formed based on governing equations of motions. In this method, the dynamic response of the system is modeled and generally, it is in matrix form with stiffness matrix and mass matrix to represent the system structure. Applying the boundary conditions and the assumption of harmonic motion the system is simplified to an eigenvalue problem where the eigenvalues are the square of the natural frequencies, and with the eigenvectors being the mode shapes. The solution of this problem is a range of discrete frequencies at which the structure will spontaneously oscillate at. Such an approach, particularly, is effective in structural dynamics due to the possibility to predict the vibrational properties accurately up to the complex shapes and material constitutions, such as those of nanocomposite beams supported with materials such as graphene oxide (GO).

4. Experimental analysis

Since the nanoparticles are not solved in water without any specific process, before producing concrete samples, GO nanoparticles are dispersed by using shaker (10 minutes using a mechanical shaker), magnetic stirrer (20 minutes at room temperature), and ultrasonic devices (40 minutes using a probe-type ultrasonic device) and finally mechanical mixer (5 minutes to ensure uniform dispersion with the cement paste) based on the amount of used nanoparticles than cement at specific times. The concrete samples ar cured at a temperature of 23 ± 2°C and relative humidity of over 95% in a standard moist curing room. In order to determine the average compressive strength of concrete, cubic samples with 51*51*51 mm dimensions were used based on ASTM C109/C109M standard and the compressive strength development process are studied for 3, 7, 14, and 28-day ages. The reduction in size to 51 mm was chosen to enable it to meet the practicalities of the experiment easier, eg: limited material availability using very expensive GO nanoparticle material and to enable the increase in the number of replication required to achieve good statistics. Although in routine testing 100 mm cubes are generally used, although in comparative studies, 51 mm cubes may be used provided they are corrected by proper factors and have been used in parallel studies involving nanoparticles of other types. The amount of GO concentration used to dispense in this research was that related to 0.02 by weight of cement otherwise known as the intended dose of the specimen preparation. These GO nanoparticles were initially suspended in distilled water in this ratio and the dispersion by sequential steps (mechanical

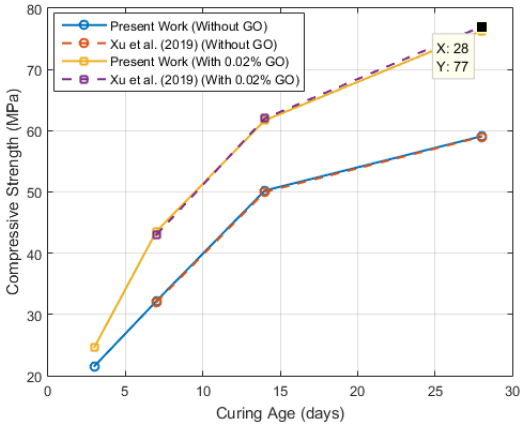

Fig. 2 The validation of this paper with Xu *et al*. (2019)

Table 1 The results of cubic samples compressive strength at different ages

Volume percent of GO	Without nanoparticles			With 0.02% nanoparticles		
	Xu *et al*. (2019)	Present work	Diff%	Xu *et al*. (2019)	Present work	Diff%
3 days	---	21.57	---	---	24.69	---
7 days	32	32.19	0.59	43	43.55	1.25
14 days	50	50.22	0.44	62	61.69	0.5
28 days	59	59.09	0.15	77	76.31	0.89

shaking, magnetic stirring, ultrasonic probe and mechanical mixing) was performed. This was to ensure that the dispersion medium retained the same concentration which would finally get into the cementitious mix. The strength developed by cubic samples are given in Table 1 and Fig. 2 and compared with Xu *et al.* (2019). Noted that the compressive strength tests are conducted based on the ASTM C109/C109M – Standard Test Method for Compressive Strength of Hydraulic Cement Mortars (Using 2-in. or [50 mm] Cube Specimens).

Fig. 2 shows the compressive strength formation in the concrete samples with the appearance of different curing ages (3, 7, 14, and 28 days), as well as the results of the present work and the study of Xu *et al*. (2019) with and without the addition of 0.02% GO nanoparticles. The final outcomes indicate that in all instances the strength was increasing with time as it should. The experimental setting and the methodology is validated in that the values of the present work closely match the literature values, particularly at higher ages. It is observed that, the addition of GO nanoparticles results in increased values of compressive strengths of all curing durations, which confirms that GO nanoparticle reinforcement has a beneficial influence on concrete performance. The differences in the datasets are also minimal (less than 1.3 percent in most cases), which just goes on to prove again that the current experimental results were accurate and replicable.

According to the numerical model elaborated, the compressive strength of the GO reinforced concrete was estimated as 78 MPa through Mori Tanaka technique using $f'_c = 4700\sqrt{E}$. Such analytical outcome shows good correspondence with the measured data in the experiments itself, which once again confirms the appropriateness of the suggested modeling model in orchestrating the mechanical response of the nanocomposite concrete. The proximity between the fundamental theory prediction and the empirical values ascertain that the model can be applied to increased parametric and structural studies.

The microstructural distribution of GO nanoparticles in the concrete matrix which is used 0.02 percent of GO by weight is portrayed in the given SEM image in Fig. 3. The microscopic observation suggests a homogenous distribution of nanoparticles in the field scope that lacks any significant clustering or agglomeration of nanoparticles at the macroscopic level. The measurements indicated, which were highlighted in th figure, affirm that the particle sizes are in the right range, that is nanometer, and are also very fine and uniform in dispersion. This homogenisation is essential in gaining the necessary mechanical enhancement which well-dispersed nanoparticles provides in the path of enhanced load transfer, crack bridging and densification of the matrix. The absence of big agglomerates proves the efficiency of the methods of dispersion applied and which are shaking, magnetic stirring, ultrasonic treatment, and mechanical mixing.

The quality of dispersion was checked on the eye and under the microscope. The sequential dispersion steps were followed by no visible clusters and sedimentation at the macroscopic scale. Better, SEM imaging of hardened

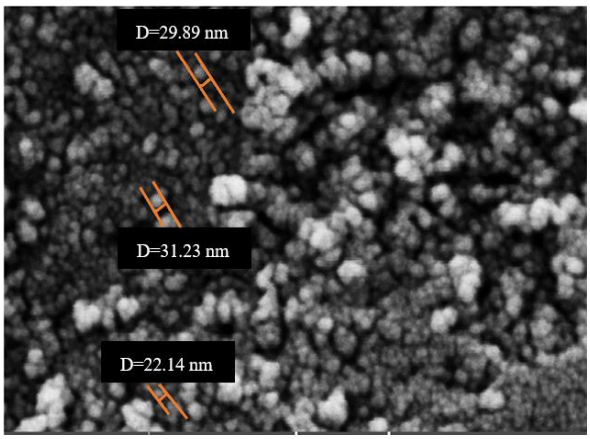

Fig. 3 SEM image for GO nanoparticles in concrete specimen

concrete samples containing 0.02% GO (Fig. 3 in paper) established that the nanoparticles present in the cement matrix were rather homogeneous and without gross clustering or large agglomerates. This offered first-hand microstructural indicators that the implemented dispersion protocol worked. Although no zeta potential measurements have been performed in the present study, the zeta potential measurements of visual inspection and SEM validation are consistent with the previously applied techniques in nanomaterial-cement studies.

5. Numerical results

An analytical model is used to determine in this chapter the natural frequency of this structure and how this frequency depends on different parameters, such as the volume fraction of GO nanoparticles, geometric properties or nanoparticle agglomeration. The elastic modulus of 20 GPa of a concrete is a very common number which has been cited in many structural engineering texts, and can be found in ASTM C469 since it is a typical value of an ordinary Portland cement concrete using a typical aggregate mix. The modulus of GO nanoparticles (250 GPa) is achieved through previous research articles that measure the characteristics of mechanical property of GO; e.g., Rafiee *et al.* (2009).

In Fig. 4, a sensitivity analysis is showing the convergence of the calculated natural frequency of a GO reinforced concrete beam employing the analytical computation and number of terms in the series. When the number of terms is going from 1 term to 10 terms, the determined frequency converges to a constant value, which proves the utility and consistency of the analytical solution. Seeing that higher-order terms have insignificant effects on the final result, the convergence trend shows that the values of the frequencies vary less than 0.1 percent relative error after about 3 terms. This trend proves that the technique used in analytical eigenvalue of the study makes a precise prediction with a sensible number of terms and aids the effectiveness of the technique applied in dynamic analysis of a nano-reinforced concrete beam.

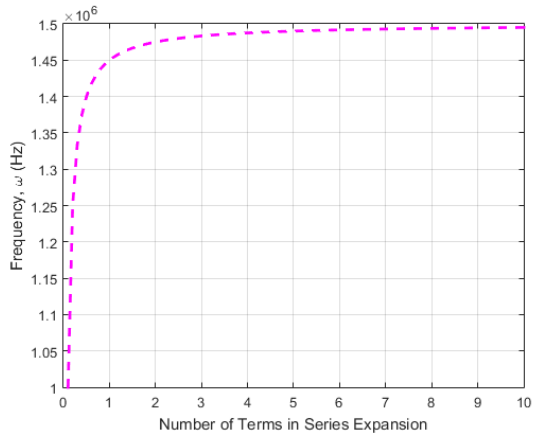

Fig. 4 The convergence of the proposed method for solution

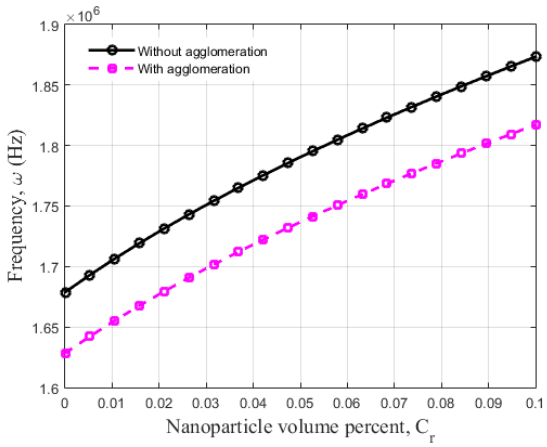

Fig. 6 The impact of agglomeration on the vibration frequency in term of GO volume percent

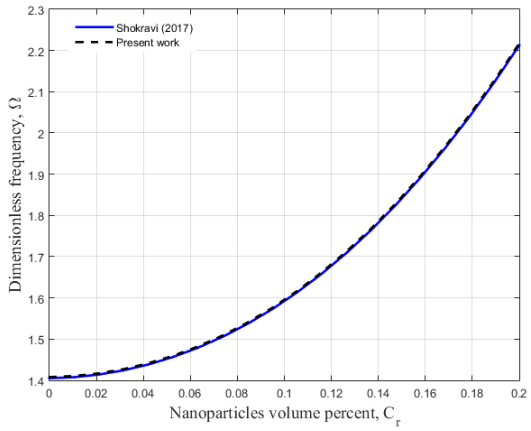

Fig. 5 The validation of this paper with Shokravi (2017)

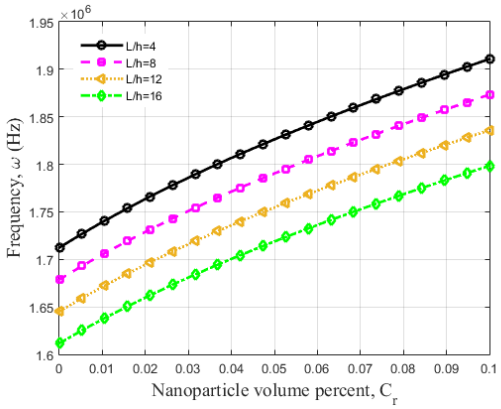

Fig. 7 The impact of length to thickness ratio on the vibration frequency in term of GO volume percent

Fig. 5 compares the present research with that of Shokravi (2017). To this end, with the assistance of zero *f* in Eq. (1) and by simplifying the theoretical model of the problem to accommodate the Euler-Bernoulli beam theory, and by using identical silica nanoparticles and equal material and geometric parameter values as the ones utilized in the mentioned paper, dimensionless frequencies observed in the present study were contrasted with those reported by Shokravi (2017). It can be seen that the results are characterized by a high level of accuracy and reliability and prove the validity of the given approach. This consent shows the congruence of the suggested methodology to the developed theories and supports the validity of the results.

The impact of agglomeration on the frequency of structure as a function of GO nanoparticles volume percent are shown in Fig. 6. At nanomaterials scale, agglomeration simply means the clumping or even clustering together of nanoparticle to each other, as a result of interparticle forces, thereby limiting their uniform dispersion throughout a matrix, and may also adversely influence the mechanical properties of the resulting composite material. In this research, these parameters are not directly measured as others but adopted after literature and parametric variation because of what has been done by other authors like Zamanian *et al.* (2017) which use them in pursuing trend and sensitivity in effective property prediction.. One can find that frequency is reduced when the agglomeration effects are considered. It could be attributed to the fact that the consideration of agglomeration effect results in reduced stiffness to the structure. The dominant influence of agglomeration effect on vibrating behaviour of structure is however major. Besides, as Cr increases, it increases the frequency as a result of high rigidity in bending.

The impact of the length-to-thickness ratio of the concrete beam on natural frequency depending on the percentage of the volume of GO (graphene oxide) nanoparticle is presented in Fig. 7. As length to thickness ratio goes up there is a visible change in the frequency. The increase in structural stiffness as the result of the alterations in the proportion of geometricals can be treated as its cause. Increased length to thickness ratio usually results in an increase in flexural rigidity of the beam which results in increased natural frequencies. Also, the addition of GO nanoparticles will help to have this behavior via enhancing the mechanical characteristics of concrete matrix e.g., Young modulus and internal damping. However, the interaction of geometric optimization and nanomaterial reinforcement has a synergistic effect and hence a greater contribution towards increasing vibrational performance of the structure. It shows that both geometrical and material

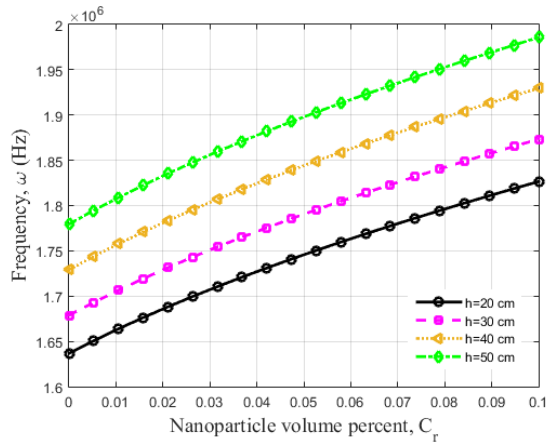

(a)

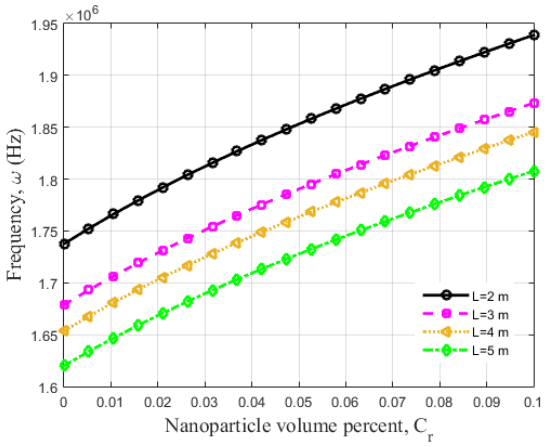

(b)

Fig. 8 (a) The impact of thickness on the vibration frequency in term of GO volume percent and (b) The impact of length on the vibration frequency in term of GO volume percent

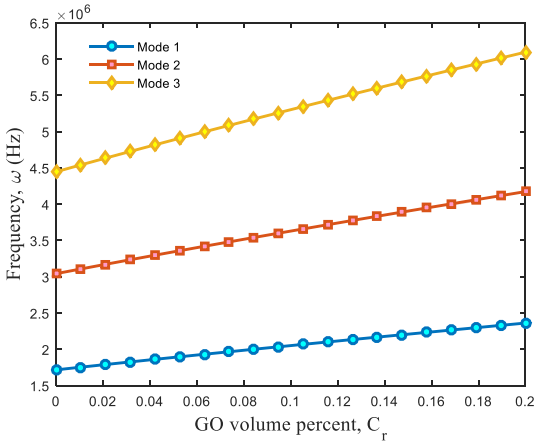

Fig. 9 The impact of mode number on the vibration frequency in term of GO volume percent

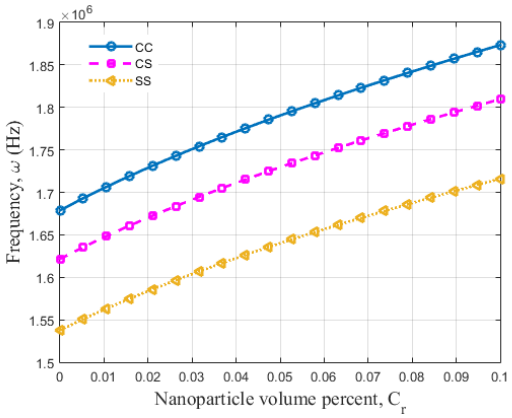

Fig. 10 The impact of boundary condition on the vibration frequency in term of GO volume percent

parameters used should be carefully adjusted according to the design of high-performance nanocomposite in concrete beam in situations where vibration control is of utmost importance.

The effect of beam length and thickness on the natural frequency is presented in Figs. 8a and 8b with respect to the change in the percentages of the volumes of GO (graphene oxide) nanoparticles. The findings show that there are two different trends: the increase in thickness will cause natural frequency to increase whereas the increase in length will cause the frequency to decrease. This is quite characterized with the classical beam theory where the natural frequency of any structure is directly proportional to the stiffness to mass ratio. As the thickness of the beam is increased, the moment of inertia increases and a structural stiffness is increased thus producing higher frequencies. Conversely, the structural flexibility also creates a deadweight effect which increases the length of the beam and decreases structural stiffness with the result that natural frequencies will be lowered. In addition, the mechanical strength of the concrete matrix is also improved during the addition of GO nanoparticle and this also has an impact on the dynamic response. The nature of the interaction between the geometric parameters and the nanoparticle reinforcement underlines the necessity of the optimization of not only the physical dimensions but also the material composition of the concrete in the effort to have desired vibrational characteristics in nanocomposite concrete constructions. The applications of such findings are particularly valuable in those aspects where frequency response control is paramount like smart infrastructures and acoustically sensitive elements.

Fig. 9 indicates the impact of mode number on the frequency as a function of volume percent of GO nanoparticles. In vibration analysis, the mode number is the particular deformation pattern or shape of a structure under a specific natural frequency, such that the higher mode numbers indicate higher frequencies and increasingly complex deformation shapes. With increase in mode number obviously the frequency is raised.

Fig. 10 shows the effect of natural frequency on volume percent nanoparticle for three different boundary conditions clamped-clamped (CC), clamped-simply supported (CS) and simply supported- simply supported (SS). The figure clearly demonstrates that increasing the percentage of nanoparticles in volume causes the increase in natural

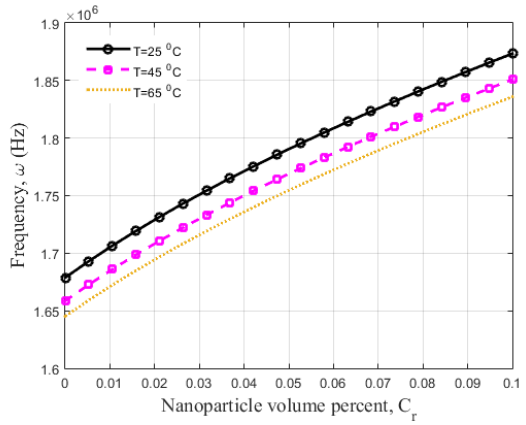

Fig. 11 The impact of temprature on the vibration frequency in term of GO volume percent

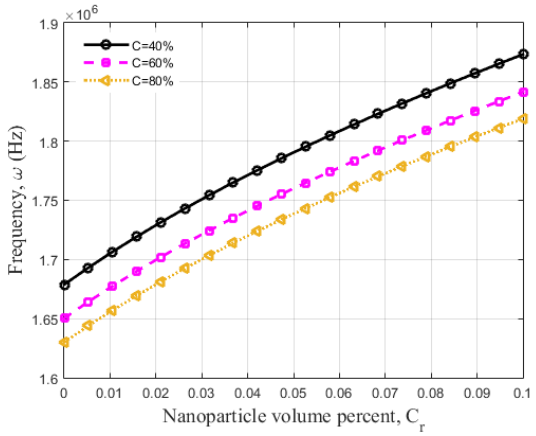

Fig. 12 The impact of moisture on the vibration frequency in term of GO volume percent

frequency under all the boundary conditions. This has been put to the fact that the structural stiffness has been significantly increased as the nanoparticles have been added and thus the mechanical properties of the composite material are also enhanced. The values of frequency are highest in the case of the first condition (CC) under study and subsequently CS and SS. Such a trend shows the effect of boundaries restrictions on the performance of vibration, with stiffer supports maturing to be stiffer and hence a higher frequency. It is concluded that dynamical response proves strongly dependent on the material composition and the support structure, a factor that should be highly considered in engineering designs that concern controlling vibration and structural acoustics.

The impact of temperature in vibration frequency of the nanocomposite concrte beams is shown in Fig. 11. The frequency of the beam reduces as temperature rises. This reduced stiffness is mostly through the freezing of the matrix material causing it to soften thus reducing the structural stiffness. Thermal expansion accompanied by increased temperatures decreases elastic modulus of the structure and decreases the resistances to vibrations in the beam.

Fig. 12 shows the effect of moisture content on the frequency of the vibration of nanocomposite concrete beams. When the moisture level rises between 40 and 80 there is a downward trend in the vibration frequency of the beam. This leakage is mainly cited to the uptake of wetness on the matrix material that results on softening of the beam. High moisture content has the effect of weakening the interfacial bonding between the nanoparticle and the cementitious matrix, which affects overall stiffness to a lower value and increases damping. As a result of this, the beam becomes less resistant to the vibrational energy, making its natural frequency to be dropped. Such behavior underlines the importance of humidity control of the environment in circumstances where vibrational efficiency and integrity are of concern, especially when deployed under outdoor or wet environments.

6. Conclusions

To sum up, the research presents an extensive assessment of the dynamic response of graphene oxide (GO) reinforced concrete beams, which proves the effectiveness of the suggested modelation method with sensitivity analysis and also confirmation of the finding of the capability of the literature. The confirmation on the accuracy and efficiency of the method is that; the convergence of natural frequency with the limited number of series terms. It has been found out that, nanoparticle agglomeration, the ratios of geometrical parameters, mode numbers, boundary effects, temperature, and moisture have a significant effect on the vibration behavior of the beam. In particular, a higher content of GO usually raises the natural frequency, because of elevated stiffness, and environmental changes, such as temperature and moisture, lower it, making the matrix softer. These observations highlight the fact that, stability demands coupling the strain versus strain rate curves and material composition, with structural parameters, to guarantee performance stability of the structure under combined dynamic loads.

The variation of the natural frequency that is anticipated to rise due to the addition of the GO nanoparticles has a significant practical consideration concerning its application on actual concrete buildings. Resonance and vibration control are important design concerns in situations like foot bridges, building floors, machine foundation and precast structural components. In confirming the stiffening of the beam reinforced with GO in raising the stiffness of the beam by both analytical and experimental results, this study shows that it is possible to avoid those critical ranges of natural frequencies. Consequently, GO-reinforced concrete might provide superior dynamic performance, and a lower possibility of resonance, and it also exhibits promising durability in a cyclic loading capacity, which makes it a good potential vibration-sensitive structural component.

Fund project

1. Key Scientific Research Project of Colleges and Universities in Henan Province, project name: Petrov-Galerkin application research of finite element method in nonlinear equation, project number: 25A110013.

References

Azandariani, M.G. and Zare, E. (2022), "Development of spectral element method for free vibration of axially-loaded functionally-graded beams using the first-order shear deformation theory", *Eur. J. Mech. A-Solids*, **96**, 104759. https://doi.org/10.1016/j.euromechsol.2022.104759.

Barbhuiya, S., Das, B.B., Adak, D. and Katare, V. (2025), "Advancements in nano-engineering of cement and concrete: a comprehensive review", *Emergent Mater.*, https://doi.org/10.1007/s42247-025-01003-0.

Chen, S.L. and Lee, S.C. (2020), "An investigation on tunnel deformation behavior of expressway tunnels", *Geomech. Eng.,* **21**(2), 215-226. https://doi.org/10.12989/gae.2020.21.2.215.

Chen, Y., Zhang, W., Zhang, Y., Liu, Z., Liu, C., Zhang, Y. and Chen, M. (2025), "A novel in-process rebar integration method for 3D printing reinforced concrete beams and performance evaluation", *Virtual Phys. Prototyp.*, **20**(1), e2536556. https://doi.org/10.1080/17452759.2025.2536556.

Cui, W., Zhao, L., Ge, Y. and Xu, K. (2024), "A generalized van der Pol nonlinear model of vortex-induced vibrations of bridge decks with multistability", *Nonlinear Dynam.*, **112**(1), 259-272. https://doi.org/10.1007/s11071-023-09047-9.

Cheng, B., Sun, Y. and Horri, A. (2025), "Application of computer approach integrating AI for nonlinear post-buckling behavior of Mindlin cut-out composite plates reinforced with FG-carbon nanotubes", *Acta Mech.*, https://doi.org/10.1007/s00707-025-04400-y.

Deng, J. and Gao, N. (2022), "Broadband vibroacoustic reduction for a circular beam coupled with a curved acoustic black hole via nullspace method", *Int. J. Mech. Sci.*, **233**, 107641. https://doi.org/10.1016/j.ijmecsci.2022.107641.

Deng, J., Ma, J., Chen, X., Yang, Y., Gao, N. and Liu, J. (2024),. "Vibration damping by periodic additive acoustic black holes", *J. Sound Vib.*, **574**, 118235. https://doi.org/10.1016/j.jsv.2023.118235.

Gao, D., Li, Z., Ding, C. and Yu, Z. (2025), "Uniaxial tensile stress-strain constitutive relationship of 3D/4D/5D steel fiber-reinforced concrete", *Constr. Build. Mater.*, **470**, 140539. https://doi.org/10.1016/j.conbuildmat.2025.140539.

Gong, B. and Li, H. (2024), "A couple Voronoi-RBSM modeling strategy for RC structures", *Struct. Eng. Mech.*, **91**(3), 239-250. https://doi.org/10.12989/sem.2024.91.3.239.

Gholami, M., Azandariani, M.G., Ahmed, A.N. and Abdolmaleki, H. (2023), "Proposing a dynamic stiffness method for the free vibration of bi-directional functionally-graded Timoshenko nanobeams", *Adv. Nano Res.*, **14**(2), 127-139. https://doi.org/10.12989/anr.2023.14.2.127.

Hamzehkhani, M.B., Zare, A., Gholami, M. and Azandariani, M.G. (2024), "Analysis of bending vibrations of a three-layered pre-twisted sandwich beam with an exact dynamic stiffness matrix", *Compos. Part C: Open Access*, **14**, 100473. https://doi.org/10.1016/j.jcomc.2024.100473.

Hong, S.K., Oh, D.W., Kong, S.K. and Lee, Y.J. (2020), "Investigation of divergence tunnel excavation according to horizontal offsets between tunnels", *Geomech. Eng*., **21**(2), 111-122. http://dx.doi.org/10.12989/gae.2020.21.2.111. .

He, D., Xu, H., Wang, M. and Wang, T. (2024), "Transmission and dissipation of vibration in a dynamic vibration absorber-roller system based on particle damping technology", *Chin. J. Mech. Eng.*, **37**(1), 108. https://doi.org/10.1186/s10033-024-01107-4.

Huang, H., Guo, M., Zhang, W. and Huang, M. (2022)., "Seismic behavior of strengthened RC columns under combined loadings", *J. Bridge Eng.*, **27**(6). https://doi.org/10.1061/(ASCE)BE.1943-5592.0001871.

Jia, H., Feng, X., Cui, B. and Liu, Z. (2025), "Design and thermal insulation simulation of nano-SiO2 foam concrete and vacuum insulation panel system for building exterior wall insulation", *Energy*, **330**, 136833. https://doi.org/10.1016/j.energy.2025.136833.

Liu, X., Tan, J. and Long, S. (2024), "Multi-axis fatigue load spectrum editing for automotive components using generalized S-transform", *Int. J. Fatigue*, **188**, 108503. https://doi.org/10.1016/j.ijfatigue.2024.108503.

Liew, K.M., Lei, Z.X., Yu, J.L. and Zhang, L.W. (2014). "Postbuckling of carbon nanotube-reinforced functionally graded cylindrical panels under axial compression using a meshless approach", *Comput. Method. Appl. M.*, **268**, 1-17. https://doi.org/10.1016/j.cma.2013.09.001.

Labaran, Y.H., Atmaca, N., Tan, M., Atmaca, K., Aram, S.A. and Kaky, A.T. (2024), "Nano-enhanced concrete: unveiling the impact of nano-silica on strength, durability, and cost efficiency", *Discov. Civ. Eng.*, **1**, 116. https://doi.org/10.1007/s44290-024-00120-9.

Niu, Y., Wang, W., Su, Y., Jia, F. and Long, X. (2024), "Plastic damage prediction of concrete under compression based on deep learning", *Acta Mech.*, **235**(1), 255-266. https://doi.org/10.1007/s00707-023-03743-8.

Prakash, V., Debono, C.J., Musarat, M.A., Borg, R.P., Seychell, D., Ding, W. and Shu, J. (2025), "Structural health monitoring of concrete bridges through artificial intelligence: A narrative review", *Appl. Sci.*, **15**(9), 4855. https://doi.org/10.3390/app15094855.

Rafiee, M.A., Rafiee, J., Srivastava, I., Wang, Z., Song, H., Yu, Z.Z. and Koratkar, N. (2009), "Fracture and fatigue in graphene nanocomposites", *Small*, **6**(2), 179-183. https://doi.org/10.1002/smll.200901480.

Setayesh, R., Hatami, S., Azandariani, M.G. and Zamani Nejad, M. (2024), "Forced vibration assessment of moderately thick carbon nanotube-reinforced composite plates", *Results Phys.*, **67**, 108034. https://doi.org/10.1016/j.rinp.2024.108034.

Shokrai, M. (2017), "Vibration analysis of silica nanoparticles-reinforced concrete beams considering agglomeration effects", *Comput. Concrete*, **19**(3), 333-338, https://doi.org/10.12989/cac.2017.19.3.333.

Song, J., Pu, Z. and Horri, A. (2025), "Energy harvesting in smart nano-engineered concrete: Bridging experimental innovations and numerical modeling for sustainable infrastructure", *Constr. Build. Mater.*, **487**, 142105. https://doi.org/10.1016/j.conbuildmat.2025.142105.

Sun, G., Kong, G., Liu, H. and Amenuvor, A.C. (2017), "Vibration velocity of X-section cast-in-place concrete (XCC) pile-raft foundation model for a ballastless track", *Can. Geotech. J.*, **54**(9), 1340-1345. https://doi.org/10.1139/cgj-2015-0623.

Su, J., Yang, H., Wang, S., Tian, J., Cai, X., Shui, F., Huang, F., Xu, Z., Zeng, Q. and Fan, Z. (2025), "Effects of dual incorporation of nano-SiO_2 and nano-$CaCO_3$ on the abrasion resistance and microstructure of concrete", *J. Wuhan Univ. Technol. - Mat. Sci. Edit.*, **40**, 509-518, https://doi.org/10.1007/s11595-025-3086-8.

Tang, C., Lu, Z., Qin, L., Yan, T., Li, J., Zhao, Y. and Qiu, Y. (2025), "Coupled vibratory roller and layered unsaturated subgrade model for intelligent compaction", *Comput. Geotech.*, **177**, 106827. https://doi.org/10.1016/j.compgeo.2024.106827.

Thai, H.T. and Vo, T.P. (2012), "A nonlocal sinusoidal shear deformation beam theory with application to bending, buckling, and vibration of nanobeams", *Int. J. Eng. Sci*., **54**, 58-66, https://doi.org/10.1016/j.ijengsci.2012.01.009.

Verma, P., Shukla, S. and Pal, P. (2025), "A comprehensive review on dispersion techniques of nano-SiO2 in concrete matrix", *Innov. Infrastruct. Solut.*, **10**, 304. https://doi.org/10.1007/s41062-025-02098-4.

Wang, J., Wu, Z., Han, J., Wang, G. and Lv, S. (2025), "Experimental study on axial load-bearing capacity of grout-

lifted compressible concrete-filled steel tube composite column.", *Tunn. Undergr. Sp. Tech.*, **165**, 106864. https://doi.org/10.1016/j.tust.2025.106864.

Wang, K., Chen, Z., Wang, Z., Chen, Q. and Ma, D. (2023)., "Critical dynamic stress and cumulative plastic deformation of calcareous sand filler based on shakedown theory", *J. Mar. Sci. Eng.*, **11**(1), 195. https://doi.org/10.3390/jmse11010195

Wu, K., Shao, Zh., Hong, S. and Qin, S. (2020), "Analytical solutions for mechanical response of circular tunnels with double primary linings in squeezing grounds", *Geomech. Eng.,* **22**(6), 509-518. https://doi.org/10.12989/gae.2020.22.6.509.

Wuite, J. and Adali, S. (2005), "Deflection and stress behaviour of nanocomposite reinforced beams using a multiscale analysis", *Compos. Struct*., **71**, 388-396, https://doi.org/10.1016/j.compstruct.2005.09.011.

Yang, G., Zhao, H., Hu, Z., Zhang, W., Xiang, Y., Jin, M. and Liu, J. (2025a), "Prediction of restrained stress for UHPC: Considering relationship between long-term and in-situ creep",. *Constr. Build. Mater.*, **484**, 141722. https://doi.org/10.1016/j.conbuildmat.2025.141722.

Yang, Q., Li, H., Zhang, L., Guo, K. and Li, K. (2025b), "Nonlinear flutter in a wind-excited double-deck truss girder bridge: Experimental investigation and modeling approach",. *Nonlinear Dynam.*, **113**(7), 6427-6445. https://doi.org/10.1007/s11071-024-10496-z.

Yang, L., Gao, Y., Chen, H., Jiao, H., Dong, M., Bier, T.A. and Kim, M. (2024),. "Three-dimensional concrete printing technology from a rheology perspective: A review", *Adv. Cement Res.*, **36**(12), 567-586. https://doi.org/10.1680/jadcr.23.00205.

Yao, Y., Zhou, L., Huang, H., Chen, Z. and Ye, Y. (2023), "Cyclic performance of novel composite beam-to-column connections with reduced beam section fuse elements", *Struct.*, **50**, 842-858. https://doi.org/10.1016/j.istruc.2023.02.054.

Yao, S., Wang, Y., Chen, F., Zhao, N., Zhang, D. and Lu, F. (2025), "Equivalent method of stiffened plates for dynamic response and damage assessment under internal blast", *Struct.*, **76**, 109046. https://doi.org/10.1016/j.istruc.2025.109046.

Zare, E., Voronkova, D.K., Faraji, O., Aghajanirefah, H., Malek Nia, H., Gholami, M. and Azandariani, M.G. (2024), "Assessment of nonlocal nonlinear free vibration of bi-directional functionally-graded Timoshenko nanobeams", *Adv. Nano Res.*, **16**(5), 473-487. https://doi.org/10.12989/anr.2024.16.5.473.

Zhai, Y., Li, S. and Zhang, X. (2025), "Vibration performance of composite doubly-curved shells embedded with damping layer", *Int. J. Struct. Stab. Dyn.*, https://doi.org/10.1142/S0219455426502652

Zhang, C., Khorshidi, H., Najafi, E. and Ghasemi, M. (2023a), "Fresh, mechanical and microstructural properties of alkali-activated composites incorporating nanomaterials: A comprehensive review", *J. Clean. Prod.*, **384**, 135390. https://doi.org/10.1016/j.jclepro.2022.135390.

Zhang, H., Xiang, X., Huang, B., Wu, Z. and Chen, H. (2023b), "Static homotopy response analysis of structure with random variables of arbitrary distributions by minimizing stochastic residual error", *Comput. Struct.*, **288**, 107153. https://doi.org/10.1016/j.compstruc.2023.107153.

Zhang, W., Lin, J., Huang, Y., Lin, B. and Liu, X. (2025), "State of the art regarding interface bond behavior between FRP and concrete based on cohesive zone model", *Struct.*, **74**, 108528. https://doi.org/10.1016/j.istruc.2025.108528.